Journal of Molecular Graphics and Modelling 53 (2014) 140–147

Contents lists available at ScienceDirect

Journal of Molecular Graphics and Modelling

journal homepage: www.elsevier.com/locate/JMGM

Distortion from planarity in arenes produced by internal rotation of one single hydroxyl hydrogen: The case of alternariol

María Garrido-Arandia, Cristina Gómez-Casado, Araceli Díaz-Perales, Luis F. Pacios*

Departamento de Biotecnología y Centro de Biotecnología y Genómica de Plantas (CBGP), Universidad Politécnica de Madrid, 28040 Madrid, Spain

ARTICLE INFO

Article history:
Accepted 15 July 2014
Available online 23 July 2014

Keywords:
Conformations
Electron density
Hydrogen bond
Aromaticity
Mycotoxins

ABSTRACT

Alternariol (AOH) and alternariol methyl ether (AME) are compounds toxic to farm animals and humans produced by ubiquitous fungi of the *Alternaria* genus. Information on chemical and physical properties of these compounds is rather scarce although their X-ray structures are known. AOH and AME are composed of three aromatic rings with three hydroxyl groups. However, the crystal structure of AOH is nonplanar whereas that of AME which differs only in one methyl group substituting one hydroxyl hydrogen is planar. By means of quantum calculations we find that the internal rotation of that single hydrogen affects the structure of AOH producing deviations from planarity near 5°. We also show that although quantum calculations predict energy differences about 5 kcal/mol between planar and perpendicular conformations of that hydrogen, its rotation has no noticeable effects on electron density properties that could indicate modifications of aromaticity features. Based upon these results, we suggest an explanation to the nonplanarity of the AOH crystal solely in terms of the spatial arrangement of molecules in the crystal interconnected through a network of hydrogen bonds involving rotatable hydroxyl hydrogens that produce distortions from planarity.

1. Introduction

Alternaria species are fungi widely distributed in the soil that can invade crops at the pre- and post-harvest stage. They are the main contaminating fungi in cereals and occur also in oilseeds, tomato, apples, citrus fruits, olives and other vegetables [1]. *Alternaria* species are known to produce more than 70 secondary metabolites which are toxic to plants and a small proportion of them have been reported to act as mycotoxins to humans and animals [2]. Alternariol (AOH, 3,7,9-trihydroxy-1-methyl-6*H*-dibenzo-[*b*,*d*]pyran-6-one) and alternariol methyl ether (AME, 3,7-dihydroxy-9-methoxy-1-methyl-6*H*-dibenzo-[*b*,*d*]pyran-6-one; Diagram 1) are the most important mycotoxins produced by fungi of the *Alternaria* genus [1,2].

AOH and AME have been shown to act as a topoisomerase poison thus inducing DNA strand breaks [3,4] and to affect estrogen receptors in mammalian cells [5] and progesterone synthesis in porcine cells in vitro [6], which can impair fertility in farm animals. In view of these effects, studies on the chemical and physical properties of AOH and AME are being urged by public organizations in charge of dealing with food safety risk assessment [1]. Information regarding their interactions with possible toxin receptors is also desirable. The structure of AOH and AME is the key basis for addressing their properties and interactions. Considering their chemical formula (Diagram 1), one should reasonably conjecture that AOH and AME are rigid, plane compounds due to their being conjugated systems with the only conformational freedom of hydroxyl groups. The crystal structure of alternariol was reported in 2010 [7] and a surprising result was that it deviates significantly from planarity (see below). This observation was explained in terms of the steric effect caused by the proximity of methyl group and the hydrogen at position 10 as the crystal structure of an analogous compound lacking methyl at position 1 (2-chloro-7-hydroxy-8-methyl-6H-dibenzo-[*b*,*d*]pyran-6-one) was indeed planar [8]. However, the crystal structure of AME was reported in 2012 [9] and it is a completely planar molecule in spite of having the same arrangement for methyl at position 1 as AOH.

The presence of hydroxyl groups in both AOH and AME allows for formation of hydrogen bonds. Besides the intramolecular hydrogen bond between the ketone oxygen and the hydroxyl at position 7, each molecule is connected to adjacent partners via intermolecular hydrogen bonds in the crystal structures of both AOH [7] and

* Corresponding author at: Departamento de Biotecnología, E.T.S. Ingenieros de Montes, Universidad Politécnica de Madrid, 28040 Madrid, Spain.
Tel.: +34 91 3364297; fax: +34 91 3366387.
E-mail address: luis.fpacios@upm.es (L.F. Pacios).

http://dx.doi.org/10.1016/j.jmgm.2014.07.011
1093-3263/

AME [9]. However, while molecules in the AOH crystal show undulated layers, the AME crystal has molecules in stacked parallel planes (see below). The possible influence of different orientations of the hydroxyl groups on the geometry and aromaticity of AOH was addressed in the unique (to the best of our knowledge) theoretical study available on alternariol up to date [10]. In that work, Scharkoi et al. obtained the geometries of the eight conformations of AOH corresponding to the 2^3 orientations of its three rotatable hydroxyl groups at 0° and 180° by means of B3LYP/6-311G(d,p) quantum calculations. Their main result was that the planarity of alternariol is dependent on these orientations with twists from coplanarity between benzene rings (dihedral C1-pyran-C10 in Diagram 1) as large as 15.7° in some cases. As for the steric effect caused by the proximity of hydrogen at position 10 to the methyl group, Scharkoi et al. found that it is noticeable in bond angles without affecting the planarity of the molecule. By using the empirical harmonic oscillator model of aromaticity [11], they also found comparable high aromaticities in the two benzene rings and a near nonaromatic character in the central pyran ring of alternariol in all the conformations considered [10].

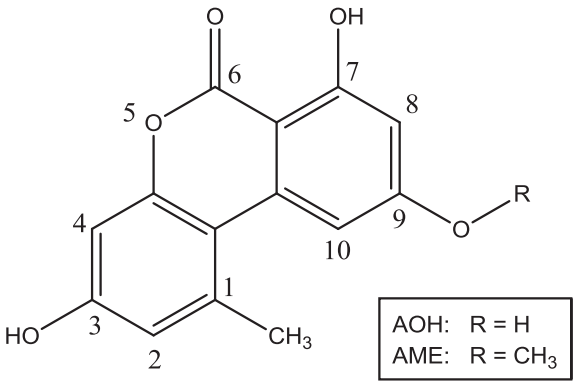

Diagram 1. Formula of alternariol (AOH) and alternariol monomethyl ether (AME).

We present in this work further quantum calculations on AOH and AME that complement the mentioned report by Scharkoi et al. Since the unique difference between these two molecules is the presence of a methyl group substituting hydrogen in the OH group

Table 1
Geometry parameters of alternariol (AOH) and alternariol methyl ether (AME) obtained in MP2 and B3LYP calculations compared with X-ray data.

Parameter	AOH				AME			
	MP2[a]	MP2[b]	B3LYP[a]	X-ray[c]	MP2[a]	MP2[b]	B3LYP[a]	X-ray[d]
Dihedrals								
C1C2C3C4	172.89	180.0	180.0	177.49	172.97	180.0	180.0	179.04
C1C2C7C8	12.01	0.0	0.0	2.42	11.91	0.0	0.0	0.94
C1O1C9C8	5.76	0.0	0.0	1.28	5.68	0.0	0.0	0.61
C3C2C7C6	0.54	0.0	0.0	2.27	0.69	0.0	0.0	0.36
C3C2C7C8	178.06	180.0	180.0	178.83	178.00	180.0	180.0	179.24
C3C4C5C6	4.09	0.0	0.0	0.08	3.70	0.0	0.0	0.21
C9C8C7C6	166.32	180.0	180.0	172.40	166.78	180.0	180.0	179.99
C9C10C11C12	4.60	0.0	0.0	2.60	4.55	0.0	0.0	0.19
C9C8C13C12	1.60	0.0	0.0	3.90	1.26	0.0	0.0	0.01
C6C7C8C13	10.63	0.01	0.0	7.92	9.97	0.0	0.0	0.36
O2C1O1C9	171.68	180.0	180.0	174.94	171.82	180.0	180.0	179.03
O2C1C2C7	178.95	180.0	180.0	176.95	178.90	180.0	180.0	178.24
O3C3C2C7	178.62	180.0	180.0	178.57	178.57	180.0	180.0	179.07
O3C3C4C5	176.84	180.0	180.0	179.77	177.04	180.0	180.0	179.17
O4C5C4C3	177.14	180.0	180.0	179.86	177.20	180.0	180.0	179.75
O4C5C6C7	179.08	180.0	180.0	179.08	178.88	180.0	180.0	179.94
O5C11C10C9	178.56	180.0	180.0	179.12	178.57	180.0	180.0	179.58
O5C11C12C13	178.62	180.0	180.0	178.65	178.61	180.0	180.0	179.97
C14C13C8C7	9.48	0.0	0.0	6.84	9.29	0.0	0.0	0.02
C14C13C12C11	177.04	180.0	180.0	176.73	177.25	180.0	180.0	179.97
H3O3C3C2	2.62	0.0	0.0	2.65	2.51	0.0	0.0	0.10
H3O2C1C2	3.67	0.0	0.0	1.45	3.59	0.0	0.0	0.86
H4O4C5C4	2.85	0.0	0.0	9.38	–	–	–	–
H5O5C11C12	1.31	0.0	0.03	10.47	1.29	0.0	0.0	5.08
H4AC4C5O4	1.08	0.0	0.0	0.45	0.86	0.0	0.0	0.16
H6AC6C7C8	6.63	0.0	0.0	0.28	6.42	0.0	0.0	0.37
H10C10C11O5	0.29	0.0	0.0	1.95	0.19	0.0	0.0	0.39
H12C12C13C14	3.98	0.0	0.0	1.91	3.90	0.0	0.0	0.06
Bond angles								
O2C1C2	124.89	125.04	125.63	125.29	124.93	125.07	125.66	125.93
O3C3C2	122.85	122.87	122.25	122.51	122.80	122.83	122.22	121.55
C8C13C14	123.95	124.56	124.83	125.07	123.93	124.48	124.77	124.14
H6AC6C7	122.52	122.99	123.12	121.61	122.63	123.06	123.12	119.20
O3H3O2	149.10	150.71	147.75	151.54	149.02	150.65	147.69	147.45
Interatomic lengths								
H3···O2	1.6888	1.6558	1.6724	1.8154	1.6901	1.6591	1.6752	1.8395
O2···O3	2.5822	2.5682	2.5639	2.6058	2.5830	2.5708	2.5661	2.5683
H6A···C14	2.3686	2.3022	2.3167	2.3558	2.3665	2.3054	2.3189	2.3729
O4—H4	0.9624	0.9689	0.9633	0.9063	–	–	–	–

Atom labeling refers to Fig. 1. Dihedral and bond angles in degrees. Interatomic lengths in Å.
[a] 6-311G(d,p) basis sets.
[b] cc-pVDZ basis sets.
[c] Ref. [7].
[d] Ref. [9].

Table 2
Geometry parameters of conformations of AOH corresponding to the internal rotation of H4 atom obtained in B3LYP/6-311G(d,p) calculations.

Parameter	H4O4C5C4 dihedral						
	0° (min)	30°	60°	90°	120°	150°	180°
Dihedrals							
C1C2C3C4	180.0	178.74	178.78	179.15	180.0	179.03	179.99
C1C2C7C8	0.0	2.03	2.03	1.07	0.54	1.74	0.01
C1O1C9C8	0.0	1.69	1.82	1.09	0.32	1.31	0.01
C3C2C7C6	0.0	1.55	1.84	1.15	0.10	0.91	0.0
C3C2C7C8	180.0	179.14	178.92	179.13	179.78	179.62	180.0
C3C4C5C6	0.0	2.53	2.93	0.85	1.66	1.93	0.0
C9C8C7C6	180.0	175.84	175.57	177.76	178.62	176.39	179.99
C9C10C11C12	0.0	0.62	0.65	0.32	0.23	0.59	0.0
C9C8C13C12	0.0	1.40	1.50	0.78	0.47	1.30	0.0
C6C7C8C13	0.0	4.47	4.73	2.41	1.44	3.85	0.01
O2C1O1C9	180.0	177.55	177.29	178.47	179.32	177.92	179.99
O2C1C2C7	180.0	179.55	179.36	179.64	179.78	179.56	180.0
O3C3C2C7	180.0	179.33	179.09	179.49	179.78	179.51	180.0
O3C3C4C5	180.0	178.63	178.52	179.52	179.32	179.05	180.0
O4C5C4C3	180.0	178.61	177.52	177.65	178.03	178.36	180.0
O4C5C6C7	180.0	177.37	176.14	177.16	178.85	179.63	180.0
O5C11C10C9	180.0	179.92	179.92	179.97	179.96	179.91	180.0
O5C11C12C13	180.0	179.75	179.73	179.86	179.90	179.75	180.0
C14C13C8C7	0.0	1.94	2.09	1.10	0.66	1.83	0.0
C14C13C12C11	180.0	178.99	178.93	179.41	179.71	179.08	180.0
H3O3C3C2	0.0	0.43	0.40	0.08	0.31	0.47	0.0
H3O2C1C2	0.0	0.30	0.22	0.02	0.36	0.55	0.0
H5O5C11C12	0.03	0.25	0.20	0.02	0.28	0.38	0.01
H4AC4C5O4	0.0	1.67	2.44	1.74	1.05	0.90	0.0
H6AC6C7C8	0.0	1.32	0.95	0.53	2.30	2.76	0.01
H10C10C11O5	0.0	0.52	0.56	0.31	0.15	0.46	0.0
H12C12C13C14	0.0	0.64	0.67	0.36	0.21	0.61	0.0
Bond angles							
O2C1C2	125.63	125.61	125.55	125.53	125.58	125.68	125.74
O3C3C2	122.25	122.25	122.31	122.40	122.32	122.13	122.05
C8C13C14	124.83	124.78	124.76	124.80	124.83	124.82	124.87
H6AC6C7	123.12	123.08	123.08	122.92	122.42	121.88	121.72
O3H3O2	147.75	147.63	147.43	147.31	147.39	147.54	147.64
Interatomic lengths							
H3···O2	1.6724	1.6762	1.6803	1.6811	1.6796	1.6793	1.6775
O2···O3	2.5639	2.5664	2.5685	2.5683	2.5674	2.5681	2.5670
H6A···C14	2.3167	2.3245	2.3270	2.3209	2.3169	2.3163	2.3060
O4—H4	1.3592	1.3645	1.3765	1.3840	1.3776	1.3649	1.3588

Atom labeling refers to Fig. 1. Dihedral and bond angles in degrees. Interatomic lengths in Å.

at position 9 (Diagram 1) and the crystal structure of AOH is nonplanar whereas that of AME is planar, we decided to study the effect produced by the rotation of that single hydroxyl on the planarity and aromaticity of alternariol. To this end, we performed B3LYP and MP2 calculations on AOH and AME and analyzed the electron density $\rho(\mathbf{r})$ of different conformations to obtain topological descriptors of $\rho(\mathbf{r})$ indicative of aromaticity effects. We show that the internal rotation of that single hydroxyl affects noticeably the planarity of the molecule without having a significant impact on $\rho(\mathbf{r})$ features indicative of aromaticity. We suggest that the difference in the planarity of the crystal structures must be attributed to the different packing of the molecules in the crystals that affect the conformation of hydroxyl groups. In line with recent reports addressing errors in geometries of aromatic molecules obtained in correlated calculations [12], we also present evidence on the effect of basis sets on MP2 geometries of AOH and AME.

2. Methods

Geometries of alternariol (AOH) and alternariol methyl ether (AME) were optimized without symmetry constraints in B3LYP/6-311G(d,p), MP2/6-311G(d,p), and MP2/cc-pVDZ quantum calculations. The stability of wavefunctions at these levels of theory was also analyzed for AOH. Geometries of conformations corresponding to the internal rotation of hydroxyl hydrogen in position 9 (Diagram 1) at 30° steps between 0° and 180° were also fully optimized in B3LYP/6-311G(d,p) calculations. Electron densities $\rho(\mathbf{r})$ were then obtained in single-point calculations at all optimized geometries in wavefunction WFN format. Geometries, stability calculations, and electron densities were computed with Gaussian 09 [13].

The localization and characterization of critical points of $\rho(\mathbf{r})$ according to the Atoms in Molecules (AIM) theory [14,15] was accomplished with EXTREME, a module of the AIMPAC package [16]. Isocontour maps of $\rho(\mathbf{r})$ were plotted from numerical grids computed with CheckDen [17]. Analysis of geometries and plots of crystal structures were performed with VESTA 3.1 [18].

3. Results and discussion

The crystal structure of AOH with the atomic labeling from X-ray data [7] and used hereafter for both AOH and AME is shown in Fig. 1. Geometry parameters selected for illustrating the planarity of these molecules as well as steric effects between methyl group and atom H6A along with geometry data of the intramolecular O2···H3—O3 hydrogen bond are listed in Table 1.

According to dihedrals gathered in Table 1, the X-ray structure of AOH exhibits nonplanar benzene rings (B and C) with twists from intra-ring planarity between 1.3° and 3.9° and greater distortions from inter-ring planarity as large as 7.6° (C6C7C8C9

Table 3
Electron density values ρ_C at critical points of the B3LYP/6-311G(d,p) $\rho(\mathbf{r})$ for conformations of AOH corresponding to the internal rotation of H4 atom.

Critical point	H4O4C5C4 dihedral						
	0° (min)	30°	60°	90°	120°	150°	180°
Ring A							
C1—C2	0.2870	0.2865	0.2856	0.2850	0.2855	0.2864	0.2868
C2—C7	0.2895	0.2901	0.2907	0.2905	0.2903	0.2906	0.2907
C7—C8	0.2658	0.2661	0.2663	0.2660	0.2658	0.2658	0.2655
C8—C9	0.3007	0.3009	0.3010	0.3010	0.3009	0.3008	0.3006
C9—O1	0.2726	0.2725	0.2721	0.2720	0.2725	0.2734	0.2739
O1—C1	0.2874	0.2874	0.2878	0.2882	0.2877	0.2867	0.2864
Ring B							
C2—C3	0.2951	0.2950	0.2950	0.2953	0.2950	0.2941	0.2935
C3—C4	0.3130	0.3130	0.3129	0.3125	0.3127	0.3139	0.3147
C4—C5	0.3138	0.3141	0.3158	0.3180	0.3182	0.3165	0.3156
C5—C6	0.3093	0.3103	0.3120	0.3120	0.3102	0.3082	0.3074
C6—C7	0.3057	0.3052	0.3043	0.3040	0.3041	0.3040	0.3037
Ring C							
C9—C10	0.3150	0.3150	0.3151	0.3151	0.3151	0.3150	0.3149
C10—C11	0.3176	0.3174	0.3174	0.3175	0.3176	0.3176	0.3178
C11—C12	0.3102	0.3101	0.3101	0.3101	0.3101	0.3101	0.3101
C12—C13	0.3089	0.3089	0.3089	0.3089	0.3089	0.3089	0.3089
C13—C8	0.2882	0.2884	0.2884	0.2883	0.2882	0.2883	0.2881
C—O bonds							
C1—O2	0.4060	0.4064	0.4070	0.4073	0.4072	0.4070	0.4068
C3—O3	0.3095	0.3092	0.3089	0.3089	0.3093	0.3095	0.3095
C5—O4	0.2887	0.2863	0.2809	0.2778	0.2806	0.2862	0.2889
C11—O5	0.2886	0.2885	0.2887	0.2888	0.2888	0.2888	0.2888
Noncovalent paths							
O2···H3	0.0514	0.0509	0.0504	0.0503	0.0505	0.0505	0.0508
C14···H6A	0.0165	0.0163	0.0162	0.0164	0.0165	0.0165	0.0167
Ring critical points							
RCP A	0.0196	0.0196	0.0196	0.0196	0.0196	0.0196	0.0196
RCP B	0.0200	0.0200	0.0200	0.0200	0.0200	0.0200	0.0199
RCP C	0.0205	0.0205	0.0205	0.0205	0.0205	0.0205	0.0204
RCP D	0.0202	0.0202	0.0201	0.0200	0.0201	0.0201	0.0201
RCP E	0.0088	0.0089	0.0088	0.0088	0.0088	0.0088	0.0088

Labeling refers to Fig. 1. Values in atomic units.

dihedral = 172.40°) or 7.9° (C6C7C8C13 dihedral). O2 atom is also out of plane by 5.1° (O2C1O1C9 dihedral = 174.9°) whereas the remaining oxygens deviate less than 1.5° from planarity. Methyl carbon C14 is also out of plane by 6.8° and benzene hydrogens in ring C (H10 and H12) twist about 2° whereas those in ring B (H4A and H6A) are coplanar. Deviations from planarity of hydroxyl hydrogens clearly illustrate their role in hydrogen bonding. Whereas H3 which is involved in the intramolecular O2···H3—O3 hydrogen bond is nearly coplanar with atoms in ring D, H4 and H5 atoms show the greatest deviations from planarity: 9.4° and 10.5°, respectively. As indicated below with regard to the spatial arrangement of molecules in crystals, all these deviations from planarity (except that of methyl group) can be understood by considering the involvement of donor (H4 and H5) and acceptor (O2) atoms in intermolecular hydrogen bonds. With the single exception of H5 which deviates from O5C11C12 plane by about 5°, all dihedrals of the X-ray structure of AME reveal a coplanar molecule.

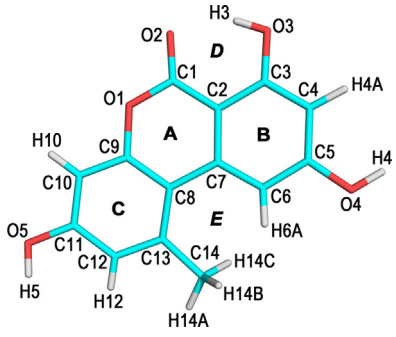

Fig. 1. X-ray structure and labeling of alternariol (AOH).

Theoretical calculations using the hybrid B3LYP method with 6-311G(d,p) basis sets predict planar geometries for AOH and AME whereas MP2 correlated calculations using the same basis sets predict nonplanar structures for both molecules. It has been reported that MP2 and CISD calculations with Pople's basis sets predict one imaginary frequency for planar benzene indicating that a nonplanar geometry is more stable than the planar one, a result also obtained for other planar arenes at different correlated levels of theory and Pople's basis sets [12,19]. It has been also suggested that rather than to deficiencies of correlation treatment in post-HF methods, the origin of the problem could be rooted on a basis set incompleteness error [19]. In line with that suggestion, a solution to the problem has been proposed by defining C—H and C—C fragments to include intramolecular counterpoise corrections [12] or alternatively, by using correlated-consistent basis sets [19]. Resorting to this latter approach, we used cc-pVDZ basis sets to perform MP2 geometry optimizations in both AOH and AME. As data in Table 1 illustrate, MP2 calculations predict now planar structures even though the smallest of the correlated-consistent basis sets is used.

However, we found correct planar structures for benzene in MP2 optimizations with both 6-311G(d,p) and cc-pVDZ basis sets (results not shown). An issue regarding the stability of wavefunctions is known to affect planar conjugate molecules [20]. In fact, there is an RHF-UHF instability with both Pople's and short correlated consistent basis sets in benzene [20] and in AOH. We found

that in alternariol the instability occurs even with cc-pVTZ basis sets (results not shown). This issue arises from the fact that unrestricted single-reference Hartree–Fock wavefunctions for singlets have a tendency to produce triplet instabilities that are artifacts of the method produced by the lack of treatment of electron correlation in conjugate systems. The problem can be dealt with by doing a stability calculation and then using the stabilized wavefunction as initial guess in the self-consistent cycle for geometry optimizations. In general, one finds that the geometry changes very little with respect to that obtained in optimizations without fixing the stability of the wavefunction. For alternariol, the differences are noticed in the second decimal place of some angles (Table S1 in Supplementary Data). On the contrary, B3LYP calculations with either type of basis sets are always stable as we checked in stability calculations with 6-311G(d,p) and cc-pVDZ basis sets in both benzene and AOH.

The calculations predict correctly bond angles O2C1C2 and O3C3C2 associated to the intramolecular O2···H3—O3 hydrogen bond but they fail at the O2···H3 distance which is predicted too short by about 0.15 Å in both AOH and AME although the experimental O2···O3 distance is well reproduced in both molecules. Since an H···O distance greater than 1.8 Å seems too large for an O···H—O hydrogen bond, it is likely that structural effects attributed to the participation of O2 in hydrogen bonds with other molecules in the crystal (see below) might explain a local distortion pulling the hydrogen atom out from O3 atom. As for geometry parameters that could reveal steric effects between methyl and H6A atom, all the calculations correctly predict C8C13C14 and H6AC6C7 angles greater than 120° in AOH although the surprisingly smaller value in AME (119.2°) is not predicted even though the interatomic H6A···C14 distance in both AOH and AME is satisfactorily given.

Since the only difference between AOH and AME is the presence of a methyl group substituting H4 atom and the crystal structure of AOH is nonplanar whereas that of AME is planar, we investigated the structural effect produced by the internal rotation of H4. To this end, we optimized geometries for conformations corresponding to H4O4C5C4 dihedral values of 30°, 60°, 90°, 120°, 150°, and 180° in B3LYP/6-311G(d,p) calculations. The results are given in Table 2 where we have selected the same geometry parameters as in Table 1. Except for 0° (structure of minimum) and 180° geometries, the remaining conformations show deviations from planarity in nearly all the dihedrals involving non-hydrogen atoms. Dihedrals between benzene rings C6C7C8C13 and C6C7C8C9 are particularly sensitive to the internal rotation of H4 showing twists from planarity as large as 4.7° and 4.4°, respectively, for the 60° conformation. Dihedrals involving C5 atom to which the rotatable hydroxyl is bonded have the following largest deviations from planarity with values C3C4C5C6 = 2.9°, O4C5C6C7 = 3.9° (176.14° in Table 2) and O4C5C4C3 = 2.5° (177.52° in Table 2) for the 60° conformation.

Although the largest twists from planarity correspond to the 60° conformation followed by 30° and 150° conformations, the maximum energy over the internal rotation of H4 corresponds to the 90° conformation which shows energy differences of 5.49, 4.49, and 4.78 kcal/mol with respect to the minimum for B3LYP/6-311G(d,p), MP2/6-311G(d,p), and MP2/cc-pVDZ calculations, respectively. While one could intuitively have predicted that the 90° conformation is a maximum in energy, the surprising result is that this conformation does not show the largest deviations from planarity. However, as it should be expected, the most stable conformation after the geometry of minimum is the 180° conformation with energy differences above the minimum of 0.96, 0.73, and 0.71 kcal/mol for results at B3LYP/6-311G(d,p), MP2/6-311G(d,p), and MP2/cc-pVDZ levels of theory, respectively. The rotation of hydroxyl is found not to have effects on geometry parameters other than dihedrals in Table 2.

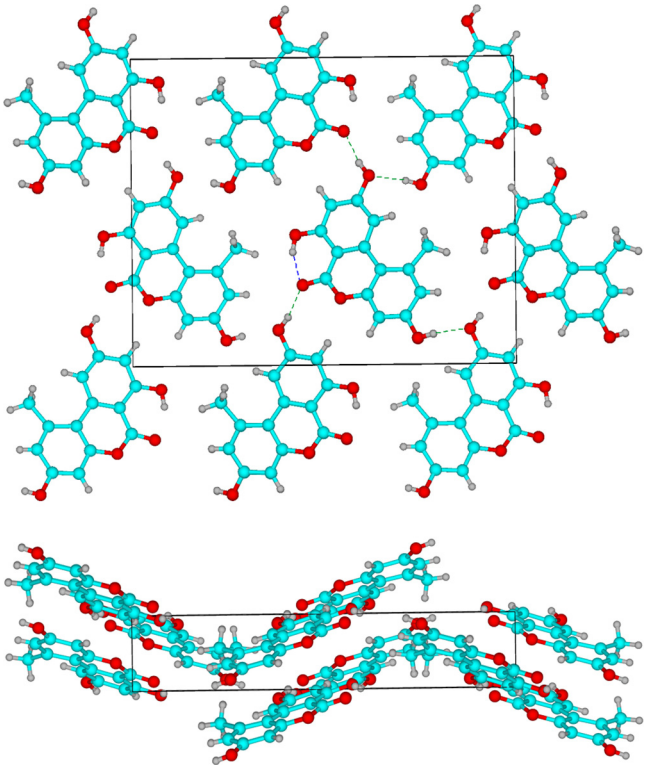

Fig. 2. View of alternariol crystal (Ref. [7]) along *b* (above) and *c* (below) crystallographic axes showing intermolecular (green dashed lines) and intramolecular (blue dashed lines) hydrogen bonds. The box indicates the unit cell. Atom color codes: C = cyan, O = red, H = gray.

According to X-ray data [7], molecules are connected in the alternariol crystal by intermolecular O—H···O hydrogen bonds into a three-dimensional network. Besides the intramolecular O3—H3···O2 bond, two intermolecular O4—H4···O2* and O5—H5···O4* H-bonds (O* means that O atoms belong to another molecule) were identified in the crystal so that each molecule is connected to four adjacent molecules (Fig. 2). In the spatial arrangement of the crystal, alternariol molecules form undulated layers in the ac plane (Fig. 2). In view of the effect that the conformation of H4 has in the planarity of AOH, it seems reasonable to assume that the nonplanar structure in the crystal is a consequence of the conformations of hydrogen atoms involved in intermolecular hydrogen bonds. In the alternariol methyl ether crystal (Fig. 3) [9], each molecule forms four bridging interactions (two O—H···O and two C—H···O hydrogen bonds) besides the intramolecular O3—H3···O2 hydrogen bond but in contrast to alternariol, the units are stacked forming planar sheets (Fig. 3) with no distortion from planarity inside each molecule.

To test whether twists from planarity produced by the internal rotation of H4 in alternariol have an effect on aromaticity, we investigated the topology of the electron density $\rho(\mathbf{r})$ on the seven conformations considered here (Table 2). The isocontours map for the geometry of minimum (Fig. 4A) shows that significant values of $\rho(\mathbf{r})$ surround both methyl group and H6A atom so that an interatomic C14···H6A bond path exists forming the corresponding ring (*E* in Fig. 4B). Since the intramolecular hydrogen bond is also a bond path (O2···H3) that gives rise to the corresponding ring (*D* in Fig. 4B), $\rho(\mathbf{r})$ shows five ring critical points (RCPs) in the planar structure of alternariol (Fig. 4B). Electron density values at critical points ρ_C and ellipticity ε values at bond critical points (BCPs) are given in Tables 3 and 4, respectively.

Electron densities at critical points of C—C bonds show rather similar values $\rho_C \sim 0.29$–0.31 a.u. in benzene rings B and C

Table 4
Ellipticity values ε at bond critical points of the B3LYP/6-311G(d,p) $\rho(\mathbf{r})$ for conformations of AOH corresponding to the internal rotation of H4 atom.

Bond critical point	H4O4C5C4 dihedral						
	0° (min)	30°	60°	90°	120°	150°	180°
Ring A							
C1—C2	0.1942	0.1914	0.1856	0.1824	0.1856	0.1910	0.1936
C2—C7	0.1905	0.1913	0.1923	0.1923	0.1925	0.1944	0.1957
C7—C8	0.1194	0.1196	0.1204	0.1209	0.1206	0.1201	0.1201
C8—C9	0.2517	0.2513	0.2511	0.2513	0.2512	0.2509	0.2510
C9—O1	0.0174	0.0175	0.0174	0.0172	0.0171	0.0169	0.0166
O1—C1	0.0152	0.0156	0.0156	0.0152	0.0155	0.0164	0.0162
Ring B							
C2—C3	0.2270	0.2261	0.2253	0.2259	0.2252	0.2225	0.2208
C3—C4	0.2529	0.2499	0.2415	0.2335	0.2352	0.2458	0.2522
C4—C5	0.2568	0.2570	0.2604	0.2659	0.2653	0.2582	0.2535
C5—C6	0.2342	0.2392	0.2471	0.2487	0.2438	0.2394	0.2380
C6—C7	0.2325	0.2279	0.2194	0.2170	0.2227	0.2295	0.2323
Ring C							
C9—C10	0.2676	0.2678	0.2681	0.2680	0.2676	0.2670	0.2666
C10—C11	0.2547	0.2546	0.2544	0.2543	0.2543	0.2545	0.2547
C11—C12	0.2325	0.2326	0.2325	0.2323	0.2323	0.2324	0.2322
C12—C13	0.2477	0.2475	0.2475	0.2478	0.2484	0.2489	0.2494
C13—C8	0.2059	0.2059	0.2057	0.2058	0.2066	0.2075	0.2076
C—O bonds							
C1—O2	0.1063	0.1065	0.1067	0.1068	0.1069	0.1071	0.1071
C3—O3	0.0022	0.0019	0.0004	0.0001	0.0017	0.0028	0.0026
C5—O4	0.0329	0.0522	0.0770	0.0872	0.0805	0.0550	0.0328
C11—O5	0.0164	0.0162	0.0159	0.0158	0.0158	0.0159	0.0160
Noncovalent paths							
O2···H3	0.0026	0.0031	0.0033	0.0031	0.0031	0.0035	0.0033
C14···H6A	2.011	2.012	2.013	2.026	1.984	1.970	2.016

Labeling refers to Fig. 1.

indicative of a nearly identical intra-ring electron distribution. In contrast, C—C bonds in ring A show slightly different ρ_C values that suggest a different electron distribution to that of rings B and C. The largest differences are found for C—O bonds: (i) intra-ring C—O bonds in the pyran moiety together with C5—O4 and C11—O5 bonds have $\rho_C = 0.27–0.29$ a.u., (ii) C3—O3 has $\rho_C = 0.31$ a.u., and (iii) C1—O2 bond has $\rho_C = 0.41$ a.u. All these values are compatible with (i) the existence of single bonds for both intra-ring C—O bonds and C—OH bonds, (ii) the known increased electron density for the C—O bond involved in an O···H—OC hydrogen bond [21,22] and (iii) the existence of a C=O double bond in the ketone group of ring A.

As for electron density values at BCPs of noncovalent paths it is helpful to recall Popelier's criteria for characterizing hydrogen bonding in AIM theory [15]. According to the first of these criteria, usual hydrogen bonds are characterized by ρ_C values in the range [0.002–0.04] a.u. A greater value as $\rho_C \sim 0.05$ a.u. for the O2···H3 path reveals thus a strong hydrogen bond interaction [15,21,22]. Interestingly, the C14···H6A path shows $\rho_C = 0.016$ a.u., a value well above the lower limit of the ρ_C range in the Popelier criterion. Since no hydrogen bonding is now involved, that relatively large electron density at the C14···H6A path illustrates the considerable sharing of electron density in ring *E* seen in Fig. 4A. The main result of ρ_C data in Table 3 concerning possible effects produced by the internal rotation of H4 is that no significant differences between conformations are noticed. With the single exception of the C5—O4 bond to which the rotatable hydrogen H4 is linked, none of differences between conformations in Table 3 is greater than 0.01 a.u.

Ellipticity at BCPs, ε, is a more sensitive descriptor of $\rho(\mathbf{r})$ to characterize the nature of bonds. Let us recall that the ellipticity is defined as $\varepsilon = (\lambda_1/\lambda_2) - 1$ where λ_1 and λ_2 are the two negative eigenvalues ($\lambda_1 \leq \lambda_2 < 0$) of the Hessian that summarize the curvature of $\rho(\mathbf{r})$ at the BCP [14,15]. The quotient $|\lambda_1|/|\lambda_2|$ measures the extent to which the electron density is elongated in one direction compared to another, both perpendicular to the interatomic line i.e., how elliptical the electron density is at a plane perpendicular to the bond path at the BCP. Defining ε as $(\lambda_1/\lambda_2) - 1$, it ranges between zero and infinity. In infinitely "thin" elliptical shapes of $\rho(\mathbf{r})$, $\lambda_2 \to 0$ and $\varepsilon \to \infty$ whereas in cylindrical shapes of $\rho(\mathbf{r})$, $\lambda_1 = \lambda_2$ and $\varepsilon = 0$. Hence, ε can be related to the π-character of a bond. For instance, the central C—C bond in butane has $\varepsilon = 0.014$, it increases to 0.176 for C—C bonds in benzene and further to 0.298 for the double bond in ethene [15].

Ellipticity values in Table 4 clearly discriminate between rings: C—C bonds in benzene rings B and C have markedly greater ε values than bonds in ring A. Assuming a greater π-character for greater ε values, it is found that inside benzene rings, C3—C4 and C4—C5 bonds (ring B) and C9—10 and C10—C11 bonds (ring C) show noticeably greater π-character than the remaining C—C bonds that have in turn greater ellipticities that bonds in pyran (ring A). This ring has in fact a clearly different nature: C—C bonds shared with benzene rings have ε values comparable to those of benzenes while C7—C8 has a lower value $\varepsilon \sim 0.120$ and C9—O1 and O1—C1 have $\varepsilon \sim 0.015–0.017$ indicative of pure single bonds. As for the remaining C—O bonds, the ketone C1—O2 bond has a greater value ($\varepsilon = 0.106$) than C—OH bonds which show $\varepsilon \to 0$ values typical of single bonds. The aromaticity picture that arises from this analysis agrees with the result obtained by Scharkoi et al. [10] who used empirical approaches to address aromaticity in their study on alternariol: rings B and C are aromatic but ring A is not. As for effects produced by the internal rotation of H4, the largest differences are found in the 90° conformation (Table 4) that has noticeable variations of ε in ring B with higher values in C4—C5 and C5—C6 bonds and lower values in C3—C4 and C6—C7 bonds as compared to both 0° and 180° conformations. However, although these variations hint to small changes in the π-character inside benzene ring B (reinforced in the two bonds of C5 atom and weakened in the two bonds next to them), the

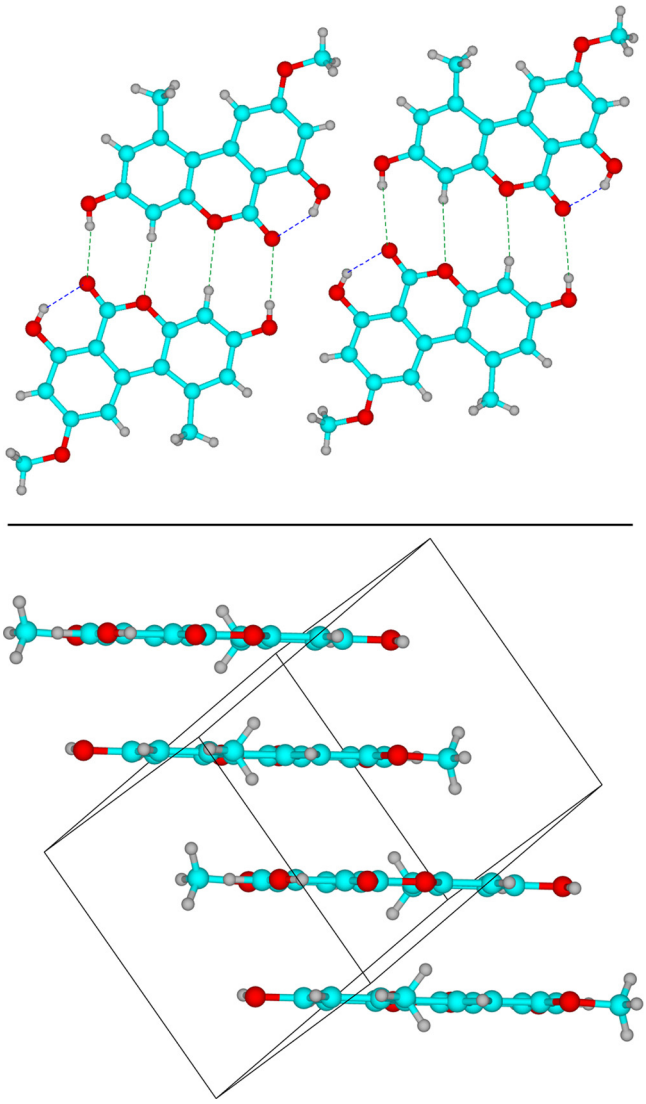

Fig. 3. View of alternariol methyl ether crystal (Ref. [9]) in the plane *ac* (above) showing intermolecular (green dashed lines) and intramolecular (blue dashed lines) hydrogen bonds and stacking of molecules along *b* axis (below). The box indicates the unit cell. Atom color codes: C = cyan, O = red, H = gray. (For interpretation of the references to color in this figure legend, the reader is referred to the web version of the article.)

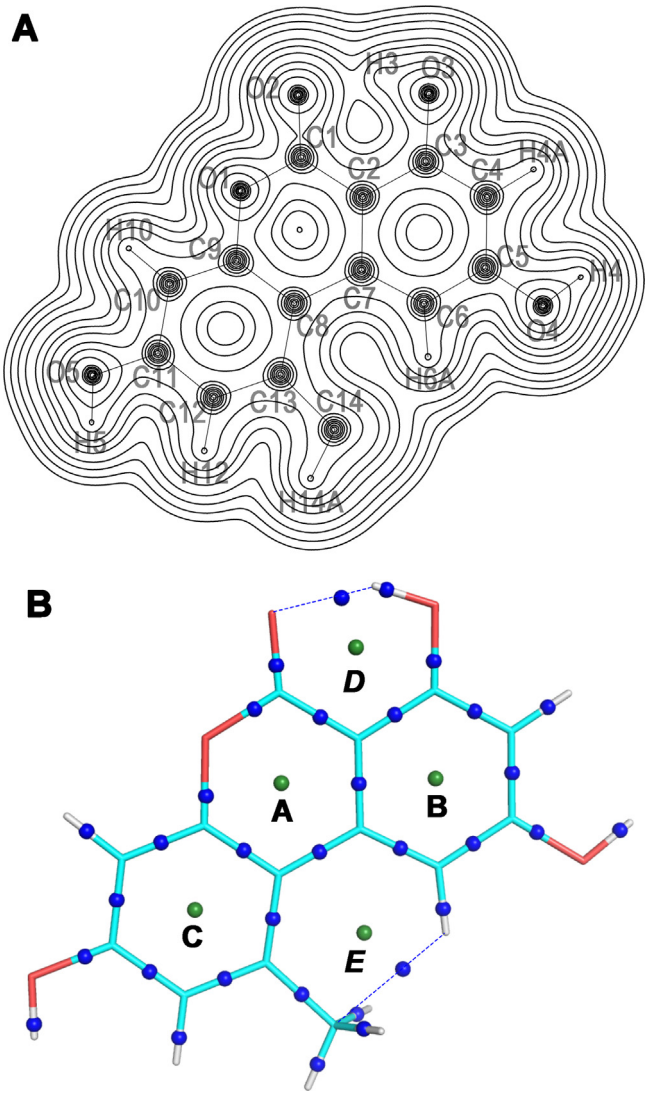

Fig. 4. Electron density $\rho(\mathbf{r})$ of alternariol at its the geometry of minimum. (A) Isocontours map at the molecular plane. The outermost contour is $\rho(\mathbf{r}) = 0.001$ a.u. and the remaining contours are 2×10^n, 4×10^n, and 8×10^n with $n = -3, -2, -1, 0, 1$ and 2. (B) Bond critical points (blue spheres) and ring critical points (green spheres) of $\rho(\mathbf{r})$. (For interpretation of the references to color in this figure legend, the reader is referred to the web version of the article.)

whole aromaticity picture is not essentially modified, not particularly in the conformations with greater deviations from planarity found in geometry optimizations (Table 2).

A final remark concerns the ellipticity in noncovalent paths. The O2···H3 path has a nearly zero ε as expected for hydrogen bonds [14,15,21,22] but the C14···H6A path has a high $\varepsilon \sim 2.0$. When a RCP and a BCP come nearer, their respective λ_2 eigenvalues tend to be equal and their respective curvatures in the direction associated to λ_2 become flatter i.e., $\lambda_2 \to 0$. Upon a slight structural change, the RCP and the BCP should merge into a degenerate critical point that has $\lambda_2 = 0$ and consequently $\varepsilon = \infty$. This point represents a singularity referred to as a bifurcation (the degenerate critical point would split up in a RCP and a BCP) point, the structure is termed a bifurcation structure and the corresponding bond is structurally unstable. A high ($\varepsilon > 1.0$) ellipticity in a bond path indicates thus a structural instability [15]. The $\varepsilon \sim 2.0$ values for the C14···H6A interatomic path suggest that this bond is unstable in the sense that a small structural modification affecting methyl or H6A atom would break the bond path.

4. Conclusions

Mycotoxins alternariol and alternariol methyl ether are composed of aromatic rings with hydroxyl groups so that one could expect planar geometries for them. However, the crystal structure of the former compound happens to be nonplanar whereas that of the latter, which differs only in one methyl group substituting one hydroxyl hydrogen, is planar. By means of quantum calculations we demonstrate that the internal rotation of this single hydrogen affects the planar structure producing deviations from planarity near 5°. Based on this result, we propose that the nonplanarity of alternariol is produced solely by the arrangement in the form of undulated layers of molecules in the crystal that involve hydrogen bonds at spatial orientations of hydroxyl groups compatible with geometry deformations found in quantum calculations. Since in the alternariol methyl ether crystal, the molecules form stacked layers in which intermolecular hydrogen bonds do not involve out of plane geometries of hydroxyls, this compound shows in the crystal a planar structure. The internal rotation of the hydroxyl hydrogen that distorts planarity occurs without noticeable effects on electron

density properties that could suggest modifications of aromaticity in alternariol even though quantum calculations predict energy differences about 5 kcal/mol between plane and perpendicular conformations of that hydrogen.

Competing interests

The authors declare that no competing interests exist.

Acknowledgments

This work was supported by the Ministry of Science and Innovation (project BIO2009-07050) and FIS-Thematic Networks and Co-operative Research Centres: RIRAAF (RD13/0014). C Gómez Casado was supported by a training Grant from the Spanish Government (FPI programme, MICINN-MINECO).

Appendix A. Supplementary data

Geometry parameters of alternariol obtained in optimizations without and with stabilization of the wave function and geometries and energies of all the structures referred to in Tables 1 and 2. Supplementary data associated with this article can be found, in the online version, at http://dx.doi.org/10.1016/j.jmgm.2014.07.011.

References

[1] European Food Safety Authority, Scientific Opinion on the risks for animal and public health related to the presence of *Alternaria* toxins in feed and food, EFSA J. 9 (2011) 2407, pp. 1–97.
[2] R. Barkai-Golan, Alternaria mycotoxins, in: R. Barkai-Golan, P. Nachman (Eds.), Mycotoxins in Fruits and Vegetables, Academic Press, San Diego, CA, USA, 2008, pp. 185–203.
[3] M. Fehr, G. Pahlke, J. Fritz, M.O. Christensen, F. Boege, M. Altemöller, J. Podlech, D. Marko, Alternariol acts as a topoisomerase poison, preferentially affecting the IIα isoform, Mol. Nutr. Food Res. 53 (2009) 441–451.
[4] C. Tiessen, M. Fehr, C. Schwarz, S. Baechler, K. Dommanich, U. Bötter, G. Pahlke, D. Marko, Modulation of the cellular redox status by the *Alternaria* toxins alternariol and alternariol monomethyl ether, Toxicol. Lett. 216 (2013) 23–30.
[5] L. Lehmann, J. Wagner, M. Metzler, Estrogenic and clastogenic potential of the mycotoxin alternariol in cultured mammalian cells, Food Chem. Toxicol. 44 (2006) 398–408.
[6] U. Tiemann, W. Tomek, F. Schneider, M. Müller, R. Pöhland, J. Vanselow, The mycotoxins alternariol and alternariol methyl ether negatively affect progesterone synthesis in porcine granulosa cell in vitro, Toxicol. Lett. 186 (2009) 139–145.
[7] D. Siegel, S. Troyanov, J. Noack, F. Emmerling, I. Nehls, Alternariol, Acta Cryst. Sect. E 66 (2010) o1366.
[8] B. Appel, N.N.R. Salch, P. Langer, Domino reactions of 1,3-bis-silyl enol ethers with benzopyrylium triflates: efficient synthesis of fluorescent 6*H*-benzo [*c*]chromen-6-ones, dibenzo [*c*,*d*]chromen-6-ones, and 2,3-dihydro-1*H*-4,6-dioxachrysen-5-ones, Chem. Eur. J. 12 (2006) 1221–1236.
[9] S. Dasari, M. Bhadbhade, B.A. Neilan, Alternariol 9-*O*-methyl ether, Acta Cryst. Sect. E 68 (2012) o1471.
[10] O. Scharkoi, K. Fackeldey, I. Merkulow, K. Andrae, M. Weber, I. Nehls, D. Siegel, Conformational analysis of alternariol on the quantum level, J. Mol. Model. 19 (2013) 2567–2572.
[11] J. Kruszewski, T. Krygowski, Definition of aromaticity based on the harmonic oscillator model, Tetrahedron Lett. 13 (1972) 3839–3842.
[12] D. Asturiol, M. Duran, P. Salvador, Intramolecular basis set superposition error effects on the planarity of benzene and other aromatic molecules: a solution to the problem, J. Chem. Phys. 128 (2008) 144108, pp. 1–5.
[13] M.J. Frisch, G.W. Trucks, H.B. Schlegel, G.E. Scuseria, M.A. Robb, J.R. Cheeseman, G. Scalmani, V. Barone, B. Mennucci, G.A. Petersson, H. Nakatsuji, M. Caricato, X. Li, H.P. Hratchian, A.F. Izmaylov, J. Bloino, G. Zheng, J.L. Sonnenberg, M. Hada, M. Ehara, K. Toyota, R. Fukuda, J. Hasegawa, M. Ishida, T. Nakajima, Y. Honda, O. Kitao, H. Nakai, T. Vreven, J.A. Montgomery Jr., J.E. Peralta, F. Ogliaro, M. Bearpark, J.J. Heyd, E. Brothers, K.N. Kudin, V.N. Staroverov, R. Kobayashi, J. Normand, K. Raghavachari, A. Rendell, J.C. Burant, S.S. Iyengar, J. Tomasi, M. Cossi, N. Rega, J.M. Millam, M. Klene, J.E. Knox, J.B. Cross, V. Bakken, C. Adamo, J. Jaramillo, R. Gomperts, R.E. Stratmann, O. Yazyev, A.J. Austin, R. Cammi, C. Pomelli, J.W. Ochterski, R.L. Martin, K. Morokuma, V.G. Zakrzewski, G.A. Voth, P. Salvador, J.J. Dannenberg, S. Dapprich, A.D. Daniels, O. Farkas, J.B. Foresman, J.V. Ortiz, J. Cioslowski, D.J. Fox, Gaussian 09, Revision A.02, Gaussian, Inc., Wallingford, CT, 2009.
[14] R.F.W. Bader, Atoms in Molecules. A Quantum Theory, Clarendon, Oxford, UK, 1990.
[15] P. Popelier, Atoms in Molecules: An Introduction, Prentice-Hall, Harlow, UK, 2000.
[16] F.W. Biegler-Konig, R.F.W. Bader, T.H. Tang, Calculation of the average properties of atoms in molecules. II, J. Comput. Chem. 3 (1982) 317–328.
[17] L.F. Pacios, A. Fernandez, CheckDen, a program to compute quantum molecular properties on spatial grids, J. Mol. Graph. Model. 28 (2009) 102–112.
[18] K. Momma, F. Izumi, VESTA 3 for three-dimensional visualization of crystal, volumetric and morphology data, J. Appl. Crystallogr. 44 (2011) 1272–1276.
[19] D. Moran, A.C. Simmonett, F.E. Leach, W.D. Allen, P.v.R. Schleyer, H.F. Schaefer, Popular theoretical methods predict benzene and arenes to be nonplanar, J. Am. Chem. Soc. 128 (2006) 9342–9343.
[20] B. Hajgató, D. Szieberth, P. Geerlings, F. De Proft, M.S. Deleuze, A benchmark theoretical study of the electronic ground state and of the singlet-triplet split of benzene and linear acenes, J. Chem. Phys. 131 (2009) 224321, pp. 1–18.
[21] O. Gálvez, P.C. Gómez, L.F. Pacios, Variation with the intermolecular distance of properties dependent on the electron density in hydrogen bond dimers, J. Chem. Phys. 115 (2001) 11166–11184.
[22] L.F. Pacios, Changes of electron properties in the formation of hydrogen bonds, in: S.J. Grabowski, J. Leszczynski (Eds.), Hydrogen Bonding – New Insights, Springer, Dordrecht, The Netherlands, 2006, pp. 109–148.